Democratic Decay of ^{6}Be Exposed by Correlations

I. A. Egorova,[1] R. J. Charity,[2] L. V. Grigorenko,[3,4,5] Z. Chajecki,[6] D. Coupland,[6] J. M. Elson,[2] T. K. Ghosh,[7]
M. E. Howard,[8] H. Iwasaki,[6] M. Kilburn,[6] Jenny Lee,[6] W. G. Lynch,[6] J. Manfredi,[2] S. T. Marley,[9] A. Sanetullaev,[6]
R. Shane,[2] D. V. Shetty,[9] L. G. Sobotka,[2] M. B. Tsang,[6] J. Winkelbauer,[6] A. H. Wuosmaa,[9]
M. Youngs,[6] and M. V. Zhukov[10]

[1]*Bogoliubov Laboratory of Theoretical Physics, JINR, Dubna 141980, Russia*
[2]*Departments of Chemistry and Physics, Washington University, Saint Louis, Missouri 63130, USA*
[3]*Flerov Laboratory of Nuclear Reactions, JINR, Dubna RU-141980, Russia*
[4]*GSI Helmholtzzentrum für Schwerionenforschung, Planckstraße 1, D-64291 Darmstadt, Germany*
[5]*National Research Center, "Kurchatov Institute," Kurchatov Square 1, RU-123182 Moscow, Russia*
[6]*National Superconducting Cyclotron Laboratory and Department of Physics
and Astronomy, Michigan State University, East Lansing, Michigan 48824, USA*
[7]*Variable Energy Cyclotron Centre, 1/AF Bidhannagar, Kolkata 700064, India*
[8]*Department of Physics and Astronomy, Rutgers University, New Brunswick, New Jersey 08903, USA*
[9]*Department of Physics, Western Michigan University, Kalamazoo, Michigan 49008, USA*
[10]*Fundamental Physics, Chalmers University of Technology, S-41296 Göteborg, Sweden*
(Received 11 August 2012; published 13 November 2012)

The interaction of an $E/A = 70$-MeV ^{7}Be beam with a Be target was used to populate levels in ^{6}Be following neutron knockout reactions. The three-body decay of the ground and first excited states into the $\alpha + p + p$ exit channel were detected in the High Resolution Array. Precise three-body correlations extracted from the experimental data allowed us to obtain insight into the mechanism of the three-body democratic decay. The correlation data are in good agreement with a three-cluster-model calculation and thus validate this theoretical approach over a broad energy range.

Introduction.—The ^{6}Be system is located beyond the proton dripline, and its ground and excited states all belong to the three-body $\alpha + p + p$ continuum. Moreover, the ^{6}Be ground state might be considered a so-called "true two-proton emitter": a system for which one-proton decay is energetically prohibited and thus should emit two protons simultaneously, as most of the strength for ^{5}Li intermediate states is inaccessible (Fig. 1). However, at large excitation energies, one expects that the decay mechanism in the three-body continuum should eventually evolve to a sequential decay process through such intermediate states. In light two-proton emitters, these intermediate states are often quite broad and hence the concept of "democratic decay" was proposed [1,2]. "Democracy" in this case means that no strong focusing in kinematical space is produced even if the intermediate states are accessible for decay; the decay mechanism remains essentially three-body in nature. The three-body decay of the ^{6}Be ground state may thus be classified as both a "true" and a "democratic" two-proton decay. The interplay and transition between the different decay mechanisms in three-body systems have been strongly debated, and they are still not completely understood [2–8]. The location of the borderline between the three-body decay dynamics (true $2p$ or democratic) and two-body dynamics (sequential decay) is not known.

In recent years, there has been a revival of interest in the ^{6}Be system [7–11] with comparative studies to two-proton

radioactive decay in ^{45}Fe [7], precise studies of correlations for the ground state [8], and the discovery of an "isovector soft dipole mode" in a charge-exchange reaction [11]. ^{6}Be is the lightest two-proton ground-state emitter and, being relatively easily accessible in experiments, could become a benchmark system for studies of two-proton emission (two-proton radioactivity in heavier nuclei). In addition, because of isospin symmetry, the two-proton correlations can shed light on the structure of the mirror neutron-halo nucleus ^{6}He [8].

In this Letter, we report on studies of the ^{6}Be continuous spectrum up to a decay energy of $E_T \sim 10$ MeV (E_T is the energy above the $\alpha + p + p$ threshold). The high-statistical-significance and high-resolution data provide a very detailed view of the evolution of the correlation patterns
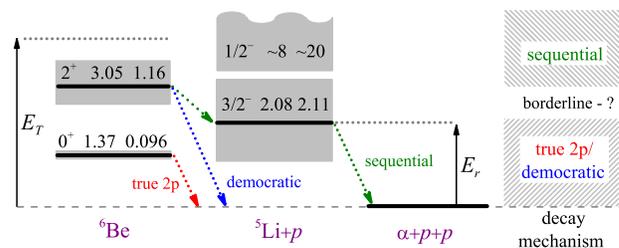

FIG. 1 (color online). Level and decay scheme for ^{6}Be and illustrations of possible decay mechanisms. The continuum states are labeled $\{J^\pi, E_r, \Gamma\}$

with excitation energy. This allows us to obtain insights into the mechanism of two-proton decay. The result is a demonstration of the counterintuitive character of the evolution of the decay mechanism with excitation energy.

Experiment.—A primary beam of $E/A = 150$ MeV ^{16}O was extracted from the Coupled Cyclotron Facility at the National Superconducting Cyclotron Laboratory at Michigan State University with an intensity of 125 pnA. This beam bombarded a ^{9}Be target, and ^{7}Be projectile-fragmentation products were selected by the A1900 separator with a momentum acceptance of $\pm0.5\%$. This ^{7}Be secondary beam had an intensity of 4×10^7 s^{-1} with a purity of $\sim90\%$. It impinged on a 1-mm thick target of ^{9}Be, creating ^{6}Be projectile-like fragments via neutron knock-out reactions.

The protons and α particles created following ^{6}Be decay were detected in the High Resolution Array [12]. For this experiment, the array consisted of 14 $\Delta E - E\,[\text{Si} - \text{CsI(Tl)}]$ telescopes located at a distance 90 cm downstream from the target and subtended zenith angles from 1.4° to 13°. Each telescope consisted of a 1.5-mm thick, double-sided Si strip ΔE detector followed by a 4-cm thick CsI(Tl) E detector. The ΔE detectors are 6.4×6.4 cm in area with each of the faces divided into 32 strips. Each E detector consisted of four separate CsI (Tl) elements, each spanning a quadrant of the preceding Si detector. Signals produced in the 896 Si strips were processed with the HINP16C chip electronics [13].

The energy calibration of the Si detectors was obtained with a ^{228}Th α-particle source. The particle-dependent energy calibrations of the CsI(Tl) detectors were achieved with $E/A = 60$ and 80 MeV beams of protons and α particles selected with the A1900 separator. An experimental ^{6}Be decay energy E_T was determined from the invariant mass of each detected $\alpha + 2p$ event minus the rest masses of the three decay products.

Theoretical model.—The dynamics of the three-body $\alpha + p + p$ continuum of ^{6}Be is described by solving the inhomogeneous three-body Schrödinger equation for wave functions (WF) with the outgoing asymptotic

$$(\hat{H}_3 - E_T)\Psi^{(+)} = \Phi_{\mathbf{q}}, \qquad (1)$$

corresponding to an approximate boundary condition of the three-body Coulomb problem. The differential cross section is expressed via the flux induced by the WF $\Psi^{(+)}$ on the remote surface S by

$$\frac{d\sigma}{d^3k_\alpha d^3k_{p_1} d^3k_{p_2}} \sim \langle\Psi^{(+)}|\hat{j}|\Psi^{(+)}\rangle|_S. \qquad (2)$$

To compare to experimental data, the calculated sevenfold-differential cross sections were used in Monte Carlo (MC) simulations of the experiment, taking into account the apparatus bias and resolution. The model is described in detail in Ref. [8] and applied in different ways in Refs. [7,11].

The source function $\Phi_{\mathbf{q}}$ for the reaction considered in this work is constructed in the approximation of a sudden removal of a neutron from ^{7}Be (transparent limit of the Serber model),

$$\Phi_{\mathbf{q}} = \int d^3r_n e^{i\mathbf{q}\mathbf{r}_n}\langle\Psi_{^4\text{He}}|\Psi_{^7\text{Be}}\rangle, \qquad (3)$$

where $\mathbf{r}_n$ is the radius vector of the removed neutron and $\mathbf{q}$ is the transferred momentum. The ^{7}Be WF is constructed in the spirit of cluster orbital shell model approximation (e.g., Ref. [14]) as an "inert" α core plus a neutron and two protons occupying $p_{3/2}$ and $p_{1/2}$ configurations with coupling $[l_j(\nu)[l_j(\pi_1)l_j(\pi_2)]_J]_{J_{^7\text{Be}}}$,

$$\Psi_{^7\text{Be}} = \Psi_{^4\text{He}}(\alpha[p_{3/2}[p_{3/2}^2]_0]_{3/2} + \beta[p_{3/2}[p_{1/2}^2]_0]_{3/2}$$
$$+ \gamma[p_{3/2}[p_{3/2}^2]_2]_{3/2} + \delta[p_{3/2}[p_{3/2}p_{1/2}]_2]_{3/2}). \qquad (4)$$

Neutron removal populates the 0^+ state in ^{6}Be for terms with coefficients $\{\alpha, \beta\}$ and populates the 2^+ state for terms with coefficients $\{\gamma, \delta\}$. The ratios α/β and γ/δ control the spin contents of the source terms in Eq. (1). From the fit of the experimental E_T distribution in Fig. 2 we obtain $\{\alpha, \beta, \gamma, \delta\} = \{0.42, 0.3, 0.49, 0.7\}$. The sensitivity of the reaction to the structure of ^{7}Be is an interesting question by itself that will be discussed elsewhere.

Complete energy-angular correlations.—Two-body decays are described by just two quantities, energy and width. For three-body decays, one also needs at least two extra continuous degrees of freedom that in this work are the energy distribution parameter ε and the angle θ_k between the Jacobi momenta $\mathbf{k}_x$, $\mathbf{k}_y$,
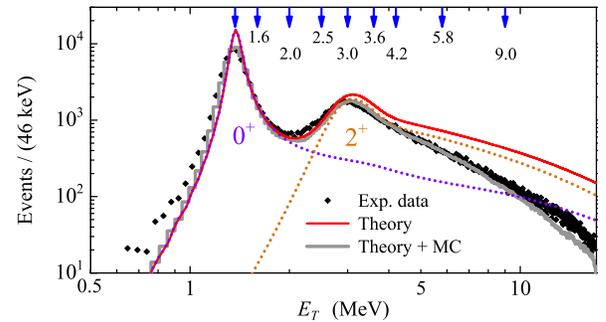

FIG. 2 (color online). Experimental invariant-mass spectrum of ^{6}Be and the fitted theoretical result. Within this work, the data points show experimental data, the solid curve shows the theoretical result, and the gray histogram shows the Monte Carlo simulation that takes into account the bias introduced by the experimental setup. To the extent that Monte Carlo simulation reproduces the experiment result, the theoretical curve can be interpreted as the reconstructed distribution. The dotted curves show the contributions of 0^+ and 2^+ states to the theoretical spectrum. The arrows indicate the boundaries of the energy bins used in this work.
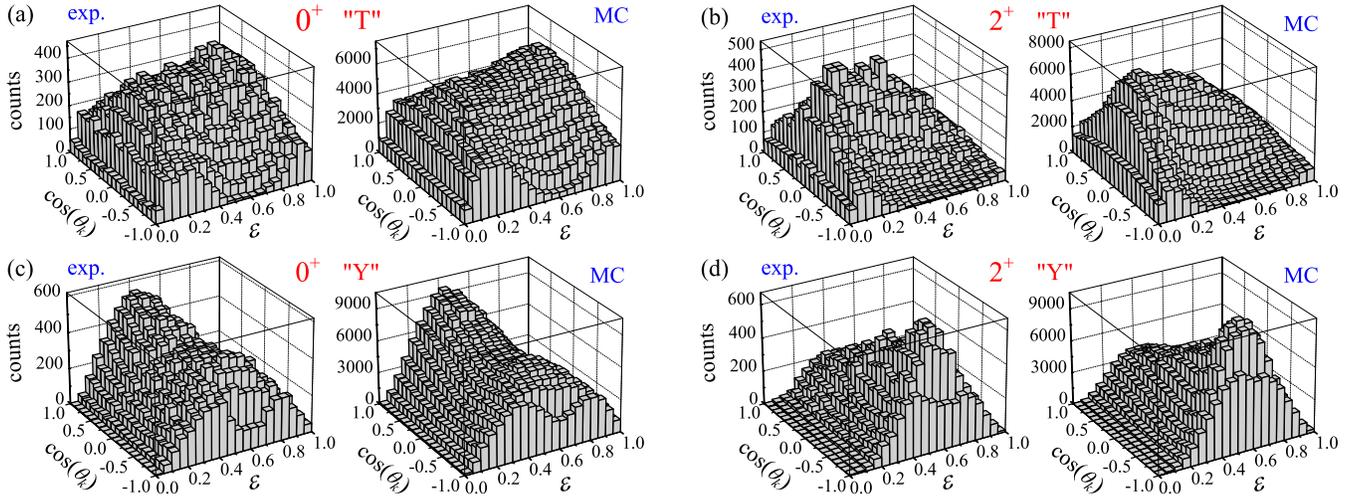
FIG. 3 (color online).   Complete energy-angular correlations for the 0^+ [(a) and (c)] and 2^+ [(b) and (d)] states of ^{6}Be. Comparison of experiment and MC simulations for Jacobi T and Y systems (upper and lower rows, respectively). The data are taken for 0.5 and 1 MeV wide bins centered on the 0^+ and 2^+ resonance peaks, respectively.

$$\varepsilon = E_x/E_T, \qquad \cos(\theta_k) = (\mathbf{k}_x \cdot \mathbf{k}_y)/(k_x k_y),$$

$$\mathbf{k}_x = \frac{A_2\mathbf{k}_1 - A_1\mathbf{k}_2}{A_1 + A_2},$$

$$\mathbf{k}_y = \frac{A_3(\mathbf{k}_1 + \mathbf{k}_2) - (A_1 + A_2)\mathbf{k}_3}{A_1 + A_2 + A_3}, \qquad (5)$$

$$E_T = E_x + E_y = k_x^2/2M_x + k_y^2/2M_y,$$

where M_x and M_y are the reduced masses of the X and Y subsystems (see, e.g., Ref. [8] for details). If we put $k_3 \rightarrow k_\alpha$, then the correlations are obtained in the "T" Jacobi system where ε describes the energy correlation in the $p - p$ channel. However, if we put $k_3 \rightarrow k_p$, then the correlations are obtained in one of the "Y" Jacobi systems where ε describes the energy correlation in the $\alpha - p$ channel.

The calculated energy-angular distributions are in excellent agreement with the experimental data for both the 0^+ and 2^+ resonances; see Fig. 3. These correlation data for the two resonance states are also in agreement with the recent results from Refs. [7–9,11] and with the older data of Refs. [1,15]. Only the data of Ref. [10] were found to be inconsistent. However, compared to all these other data sets, the present data have the highest statistical significance and thus provide the best validation of the theoretical model. In addition to the present high-statistical-significance data, we are able to explore the evolution of the correlations on and off resonance.

Evolution of energy distribution between two protons.— Figure 4 shows the evolution of the distribution of relative energy between two protons with E_T. There is a qualitative difference between the distributions for the 0^+ [Figs. 4(a) and 4(b)] and 2^+ [Figs. 4(d) and 4(e)] states. In addition, the small-E_{pp} region for $p - p$ motion becomes enhanced with increasing E_T for the 0^+ state. This result

is unexpected as the $p - p$ final-state interaction (FSI) is generally considered to be a predominantly low-energy phenomenon, but this trend is also confirmed in the calculations. For the first time, we can see the evolution of the distributions in the transition-energy region [Fig. 4(c)] characterized by strong $0^+/2^+$ state mixing. For the energy region covering the 2^+ state and beyond [Figs. 4(d)–4(f)], the energy distributions demonstrate stable shapes far beyond the 2^+ peak [Fig. 4(f)], a result again confirmed in the calculations.
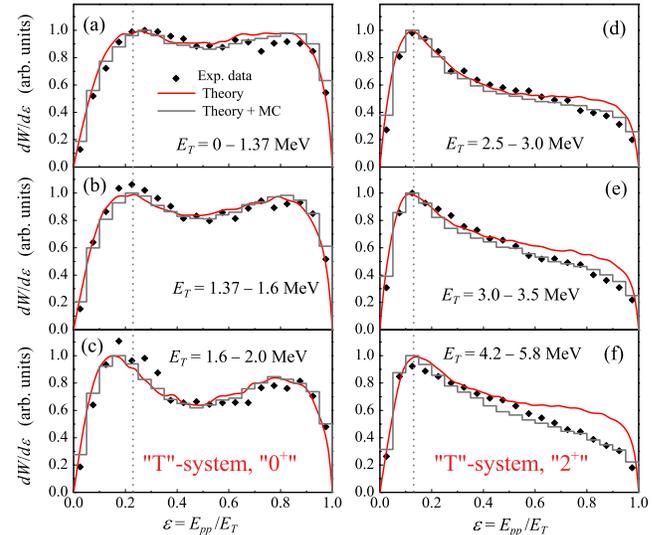

FIG. 4 (color online).   Evolution of energy distribution in the Jacobi T system (between two protons) with the decay energy. The left and right columns show the energy ranges where the 0^+ and 2^+ states dominate. Vertical dotted lines are shown to help one evaluate the shift or lack of shift in the peak location between different panels. See the caption of Fig. 2 for explanation of symbols and curves.
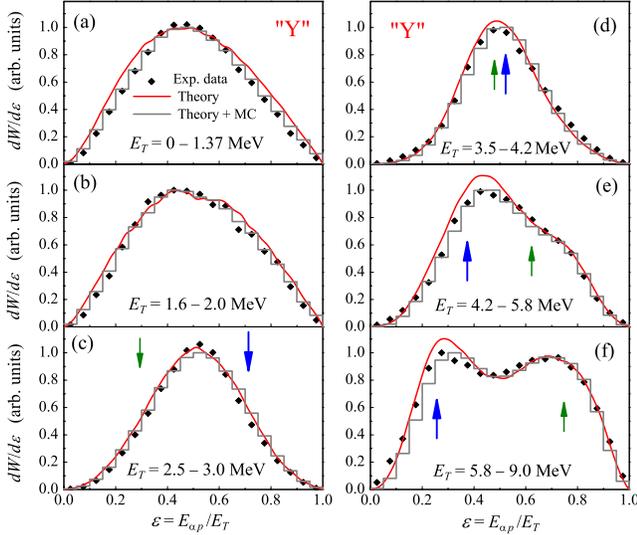
FIG. 5 (color online).   Evolution of the energy distribution in the Jacobi Y system (relative energy between the alpha and one of the protons) with energy E_T. Arrows indicate the positions of the ^{5}Li ground-state resonance in the three-body energy window. See the caption of Fig. 2 for explanation of symbols and curves.

Evolution of energy distribution between alpha and proton.—There is a widespread belief that as soon as the intermediate state becomes energetically accessible, the decay mechanism changes over from three-body decay to a sequential decay through this resonance. To see what happens in reality, let us consider the energy correlation in the $\alpha - p$ channel, which should reflect the ^{5}Li ground-state resonance in the case of sequential decay.

We can see in Figs. 5(a) and 5(b) that at low E_T, the shapes of the energy distribution in the Jacobi Y system have a relatively broad bell-like profile typical for true $2p$ decay [2]. However, as E_T increases, the profile first becomes significantly narrower. This narrowing happens exactly when the ^{5}Li ground-state resonance enters the decay window; Fig. 5(c). The location of sequential-decay strength to the centroid of the ^{5}Li resonance, $E_{\alpha p} = E_r(^5\text{Li})$ and $E_{\alpha p} \approx E_T - E_r(^5\text{Li})$, where the concentration of strength might intuitively be expected, is indicated in Fig. 5 by large blue and small green arrows, respectively. It seems that for $E_T < 2E_r(^5\text{Li})$, the availability of the two-body $\alpha - p$ resonance for sequential decay does not lead to correlation patterns that one might consider typical of sequential decay with two peaks or a peak plus a shoulder. Significant evidence for such sequential correlations are only observed when $E_T \gtrsim 2E_r(^5\text{Li}) + \Gamma(^5\text{Li})$.

Let us now turn to the energy correlation at high E_T values $(5.8 < E_T < 9.0 \text{ MeV})$; Fig. 5(f). The ^{5}Li energy correlation is very evident here with peaks located at the energies indicated by the two arrows. However, if sequential decay is the only process here, then the *angular* correlations should be completely defined by angular-momentum coupling. The predicted angular
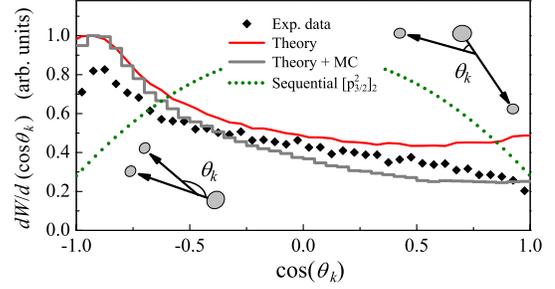

FIG. 6 (color online).   Angular distribution in the Jacobi Y system for the $E_T = 5.8$–9 MeV bin.

distribution corresponding to sequential decay via $[p_{3/2} \otimes p_{3/2}]_2$ coupling (dotted curve) is compared to the corresponding experimental data in Fig. 6. In contrast to this prediction, the experimental distribution has a strong asymmetry with a focusing of the two protons at small relative angles. Technically, such asymmetry cannot exist for pure sequential decay and must be connected with an interference between odd and even parity configurations (say of $[p^2]$ with $[sd]$ configurations in ^{6}Be). Physically, it is clear that the peak at $\cos(\theta_k) \sim -1$ is connected with $p - p$ FSI present in a realistic Hamiltonian [Eq. (1)].

A more complete picture of the decay is obtained by studying the joint energy-angular distribution of Fig. 7. This distribution contains regions clearly identifiable with $p - p$ and $\alpha - p$ FSIs and, in addition, a broad transition region. Each of these regions is responsible for roughly one-third of the events and is also present in the theoretical distribution. This agreement with the theoretical distribution strongly suggests that these features do not originate from a background of $\alpha + p + p$ events that are not associated with ^{6}Be decay. Even at such a high excitation energy, the decay is therefore not purely sequential, and the contributions of the different decay mechanisms cannot be completely disentangled. The democracy of the decay is preserved in the sense that different parts of the kinematical space have comparable populations.
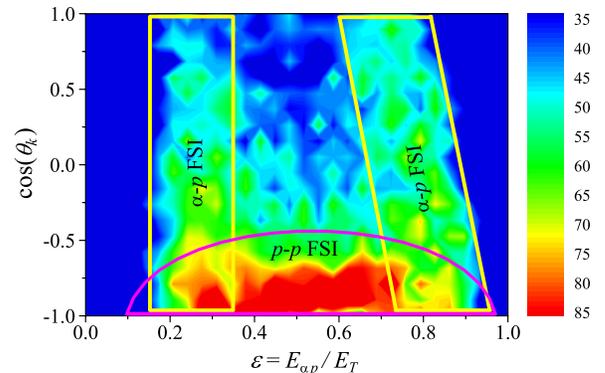

FIG. 7 (color online).   Experimental joint energy-angular distributions in the Jacobi Y system for the $E_T = 5.8$–9 MeV bin. The legend shows the number of events in each element the 30×20 grid.

Discussion.—The mechanism of three-body decays in nuclei is often discussed in terms of either the "diproton" or "sequential" decay mechanisms. The present data demonstrate two results which can be seen as paradoxical and reflect the complexity of the problem:

(i) It is now well established that the pure diproton decay mechanism is not a good picture for the $2p$ decay (Ref. [2] and references therein). However, this does not mean that the $p - p$ final-state interaction is absolutely not important for the formation of correlation patterns in such decays. In such a context then, diprotons are expected to be important for the lowest energies. However, in ^{6}Be decay there is a very clear indication that the formation of the low-energy $p - p$ correlation is enhanced as the decay energy increases. It is also more pronounced in the excited 2^+ state compared to the ground 0^+ state.

(ii) In ^{6}Be, the accessibility of the broad intermediate states in the energy window of the three-body decay first leads to what appears as a *suppression of the sequential decay mechanism* in favor of three-body democratic dynamics. Only at decay energies $E_T \gtrsim 2E_r(^5\text{Li}) + \Gamma(^5\text{Li})$ do the signs of sequential decay become visible in the correlation patterns. However, even at such energies, the actual mechanism is a complex mixture of contributions of $\alpha - p$ and $p - p$ final-state interactions, which cannot be disentangled. Some indications for this decay complexity were found in Ref. [2] based on simplified theoretical models. Now we have a strong confirmation of this finding. This establishes the validity of democratic decay as an appropriate description of the decay mechanism in a much broader energy range than ever expected.

Conclusions.—High-statistical-significance and high-resolution three-body correlation data were obtained for ^{6}Be decay over a broad range of decay energies. These experimental results are reproduced by the three-cluster model. The data elucidate the mechanism of democratic decay and emphasize the paradoxical and rather complex nature of three-body decay. They completely devalue the simplistic ideas of sequential and diproton decay in favor of complex three-body dynamics.

[1] O. V. Bochkarev, L. V. Chulkov, A. A. Korsheninniicov, E. A. Kuz'min, I. G. Mukha, and G. B. Yankov, Nucl. Phys. **A505**, 215 (1989).

[2] M. Pfützner, L. V. Grigorenko, M. Karny, and K. Riisager, Rev. Mod. Phys. **84**, 567 (2012).

[3] B. V. Danilin, M. V. Zhukov, A. A. Korsheninnikov, L. V. Chulkov, and V. D. Efros, Yad. Fiz. **46**, 427 (1987) [Sov. J. Nucl. Phys. **46**, 225 (1987)].

[4] F. C. Barker, Phys. Rev. C **68**, 054602 (2003).

[5] B. Blank and M. Ploszajczak, Rep. Prog. Phys. **71**, 046301 (2008).

[6] R. Alvarez-Rodriguez, H. O. U. Fynbo, A. S. Jensen, and E. Garrido, Phys. Rev. Lett. **100**, 192501 (2008).

[7] L. V. Grigorenko *et al.*, Phys. Lett. B **677**, 30 (2009).

[8] L. V. Grigorenko *et al.*, Phys. Rev. C **80**, 034602 (2009).

[9] R. J. Charity *et al.*, Phys. Rev. C **82**, 041304 (2010).

[10] P. Papka *et al.*, Phys. Rev. C **81**, 054308 (2010).

[11] A. S. Fomichev *et al.*, Phys. Lett. B **708**, 6 (2012).

[12] M. S. Wallace *et al.*, Nucl. Instrum. Methods Phys. Res., Sect. A **583**, 302 (2007).

[13] G. L. Engel, M. Sadasivam, M. Nethi, J. M. Elson, L. G. Sobotka, and R. J. Charity, Nucl. Instrum. Methods Phys. Res., Sect. A **573**, 418 (2007).

[14] M. V. Zhukov, A. A. Korsheninnikov, and M. H. Smedberg, Phys. Rev. C **50**, R1 (1994).

[15] D. F. Geesaman, R. McGrath, P. Lesser, P. Urone, and B. VerWest, Phys. Rev. C **15**, 1835 (1977).